



4th IASPEI / IAEE International Symposium:

Effects of Surface Geology on Seismic Motion

August 23–26, 2011 • University of California Santa Barbara

STRONG MOTION ESTIMATION AT THE MATSURUBE BRIDGE FOR THE 2008 IWATE-MIYAGI NAIRIKU EARTHQUAKE BASED ON EMPIRICAL SITE AMPLIFICATION AND PHASE EFFECTS

Yoshiya HATA
R&D Center, Nippon Koei Co., Ltd.
Tsukuba, Ibaraki 3001259
JAPAN

Atsushi NOZU
Port and Airport Research Institute
Yokosuka, Kanagawa 2390826
JAPAN

Susumu NAKAMURA
Nihon University
Koriyama, Fukushima 9638642
JAPAN

ABSTRACT

The Maturube Bridge, which is located near the epicenter of the 2008 Iwate-Miyagi Nairiku, Japan, Earthquake (Mj7.2) collapsed due to the failure of the ground behind the abutment. In order to analyze the collapse mechanism, it is very important to evaluate the strong seismic motion at the bridge site with high accuracy. First of all, aftershock observations and microtremor measurements were carried out at the bridge site in this study. Next, site effects at the left and right bank of the bridge were evaluated based on the aftershock records. Finally, seismic waveforms at the Maturube Bridge during the 2008 Iwate-Miyagi Nairiku Earthquake were estimated based on empirical site amplification and phase effects. The estimated seismic motions will be useful for a rational safety assessment of a highway bridge.

INTRODUCTION

An earthquake of JMA magnitude 7.2 hit an inland volcanic mountain area in the north of Japan on June 14, 2008 (see Fig.1). The earthquake was named “the 2008 Iwate-Miyagi Nairiku Earthquake”. A total of 23 people were dead or missing due to the earthquake, which also caused many landslides, debris flows and creation of natural dams. The Maturube Bridge shown in Photo. 1 and Fig. 2, which is located near the epicenter of the earthquake, collapsed due to the failure of the ground behind the abutment. In order to analyze the collapse mechanism, it is very important to evaluate the strong seismic motion at the bridge site with high accuracy. In this paper, strong motion estimation at the bridge site was carried out using the site effects substitution method (Hata *et al.*, 2011).

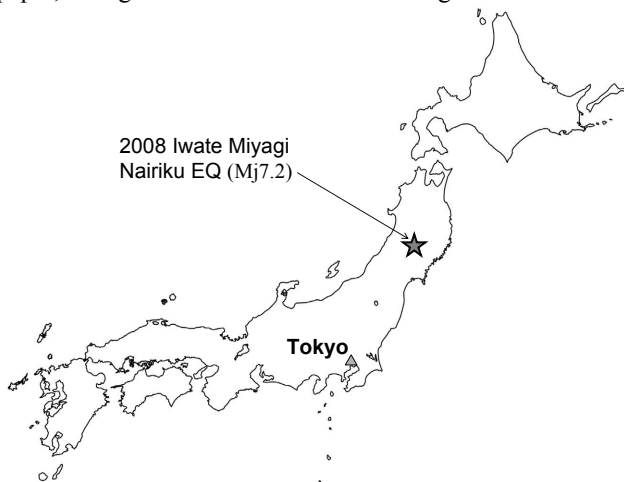


Fig. 1. The location of the 2008 Iwate-Miyagi Nairiku EQ.



Photo. 1. Collapse of the Maturube Bridge.

First of all, aftershock observations and microtremor measurements were carried out at the bridge site. Next, site effects at the left and right bank of the bridge were evaluated based on the aftershock records. Finally, seismic waveforms at the Maturube Bridge during the 2008 Iwate-Miyagi Nairiku Earthquake were estimated considering the evaluated site effects.

MICROTREMOR MEASUREMENT AND AFTERSHOCK OBSERVATION

Microtremor Measurement

Microtremor measurement was carried out in the left bank (L-1~3) and right bank (R-1~3) of the Maturube Bridge as shown in Fig. 3. The microtremor H/V spectra are shown in Fig. 4. For details of the calculation of the microtremor H/V spectrum, refer to Hata *et al.* (2010). Although at a first glance the microtremor H/V spectra at the left bank and the right bank resemble to each other, a closer look to Fig.4 reveals a slight difference, including a lower peak frequency for the right bank. Therefore, aftershock observation was conducted both at the left bank and the right bank.

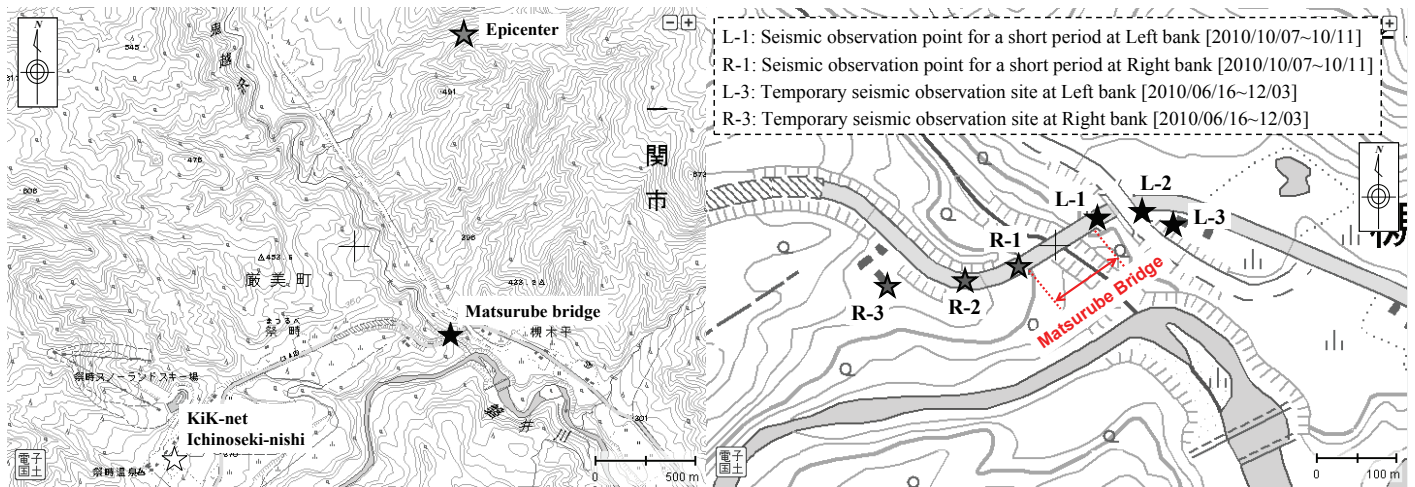


Fig. 2. The location of the epicenter and the Maturube Bridge.

Fig. 3. The microtremor measurement points.

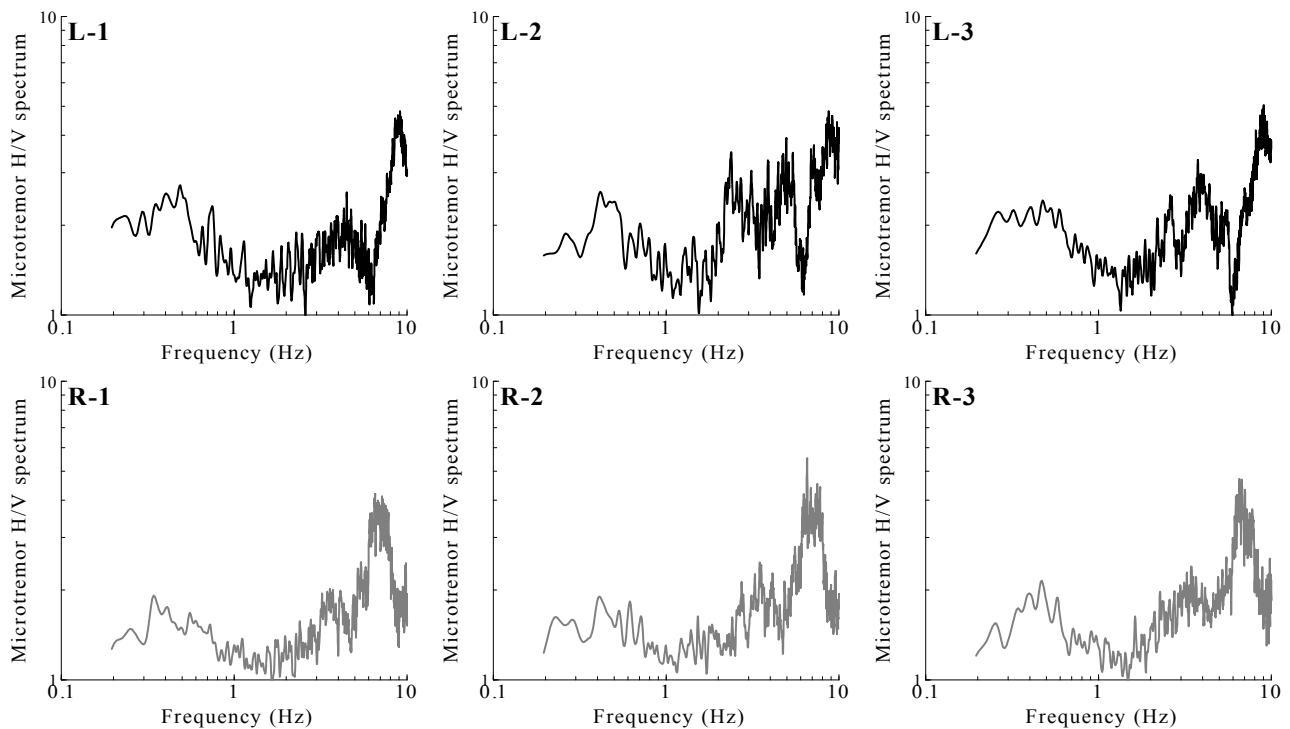


Fig. 4. The microtremor H/V spectra.

Seismic Observation

As shown in Fig. 3, temporary seismic observation sites were created at L-3 and R-3, where commercial power supply was available. The observation was conducted for about 6 months. These sites, however, were not so close to the bridge as the microtremor measurement points L-1 and R-1. Therefore, a short-period seismic observation was conducted at L-1 and R-1 for 5 days, within the limitation of power supply from battery, to examine the appropriateness of L-3 and R-3 as temporary stations.

Table 1 is the list of the observed earthquake events. EQ-01~07 are moderate earthquakes which occurred outside the source region of the 2008 main shock, and were used for the evaluation of the site amplification factor at the Maturube Bridge. The source parameters of the main shock, Aftershock 1 and Aftershock 2 are listed in Table 2. The hypocenters and earthquake mechanisms of the main shock, Aftershock 1 and Aftershock 2 are shown in Fig. 5. Aftershock 1 was used for the evaluation of the site phase effect at the Maturube Bridge because of its close location to the main shock (Hata *et al.*, 2011). Furthermore, the earthquake mechanisms of the main shock and Aftershock 1 are similar to each other. Because Aftershock 2 is the only event which was recorded at L-1 and R-1, its records were used for the evaluation of the validity of the temporary seismic observation sites (L-3 and R-3). Fig. 6 shows the observed acceleration waveforms at the ground surface of L-1, L-3, R-1 and R-3 due to Aftershock 2. In Fig. 6, the difference of seismic waveforms between the left bank and right bank can be confirmed. However, the seismic waveforms and peak accelerations at L-1 and L-3 do not differ significantly. Similarly, one cannot find significant difference in the seismic waveforms and peak accelerations at R-1 and R-3. Fig. 7 shows acceleration Fourier spectra with a Parzen window with a bandwidth of 0.05 Hz of the observed records shown in the Fig. 6. In Fig.7, the similarity of the Fourier spectra in the left bank (L-1&L-3 sites) or the right bank (R-1&R-3 sites) can be confirmed for all 3 components. These results suggest the validity of the location of the temporary seismic observation sites (L-3 and R-3).

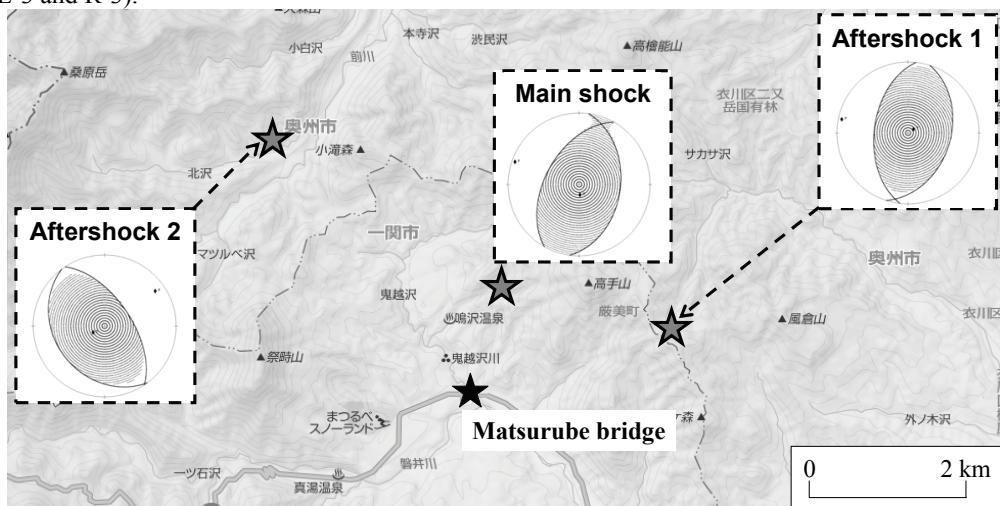


Fig. 5. The location of the main shock, Aftershock 1 and Aftershock 2.

Table 1. The list of observed earthquakes.

Year/Month/Day	Hour:Min.	Source region	JMA Magnitude
2010/06/29	07:24	Iwateken-engan-nambu (EQ-01)	Mj4.3
2009/07/04	04:33	Iwateken-nairiku-nambu (Aftershock 1)	Mj5.2
2009/07/05	06:55	Iwateken-oki (EQ-02)	Mj6.4
2010/07/27	08:31	Miyagiken-oki (EQ-03)	Mj5.3
2010/08/10	14:50	Sanriku-oki (EQ-04)	Mj6.3
2010/08/31	11:30	Akitaken-oki (EQ-05)	Mj4.9
2010/09/13	14:47	Aomoriken-toho-oki (EQ-06)	Mj5.8
2010/09/29	03:35	Iwateken-engan-hokubu (EQ-07)	Mj4.1
2010/10/08	15:53	Miyagiken-hokubu (Aftershock 2)	Mj4.2

	Used for the evaluation of amplification characteristics
	Used for the evaluation of phase characteristics
	Used for the validation of the location of temporary stations

Table 2. Parameters for the main shock and aftershocks.

	Date	Time (hour/min.)	Latitude* (deg.)	Longitude* (deg.)	Depth* (km)	M_j^*	M_0^{**} (Nm)	(strike, dip, rake)** (deg.)
Main shock	2008/06/14	08:43	N 39.028	E 140.880	8	7.2	2.72E+19	(209, 104, 51)
Aftershock 1	2010/07/04	04:33	N 39.023	E 140.912	7	5.2	4.13E+16	(186, 83, 51)
Aftershock 2	2010/10/08	21:16	N 39.048	E 140.842	6	4.4	3.70E+15	(326, 92, 60)

* after JMA

** after F-net (www.fnet.bosai.go.jp)

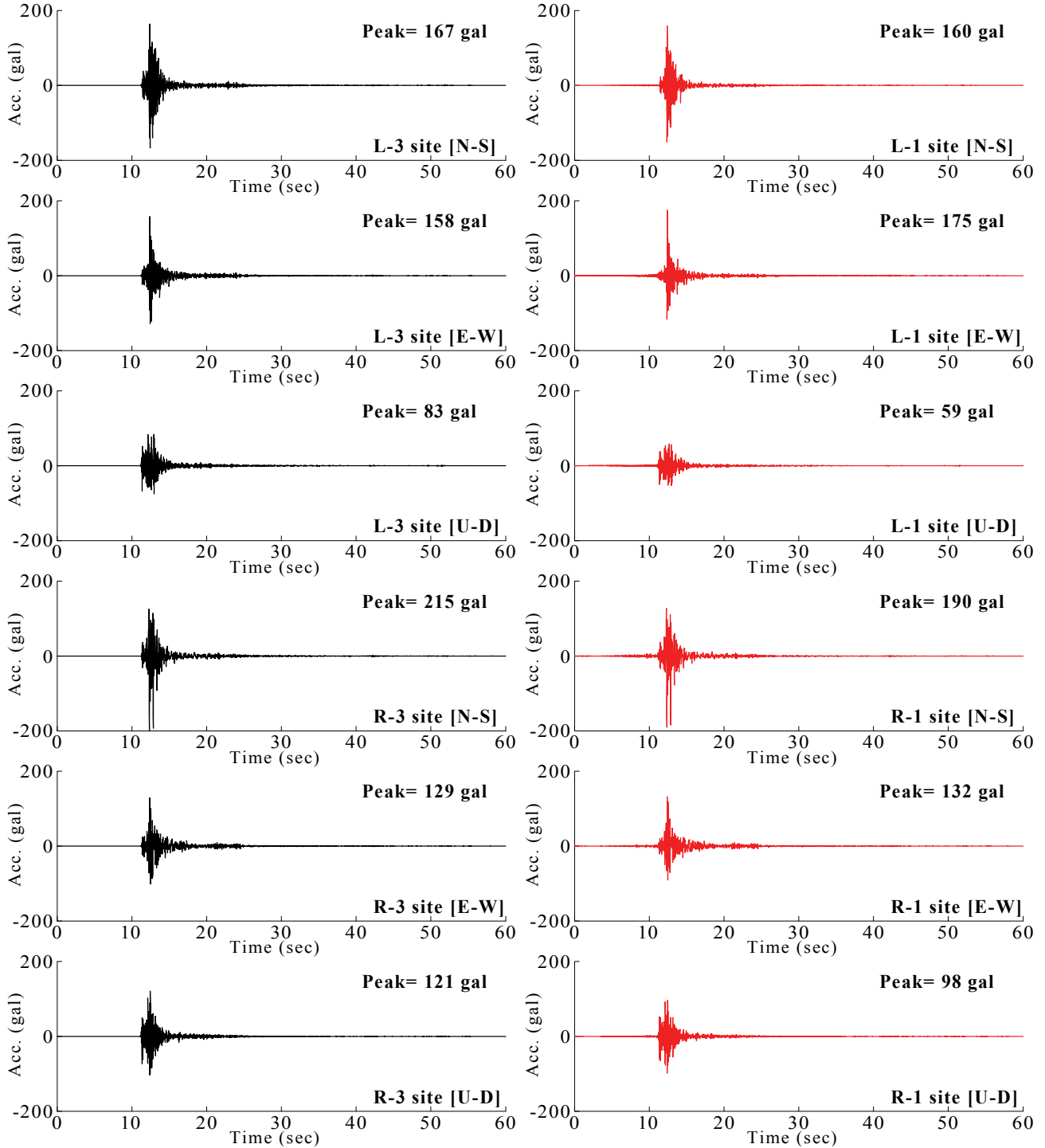


Fig. 6. Observed acceleration waveforms at the ground surface due to Aftershock 2.

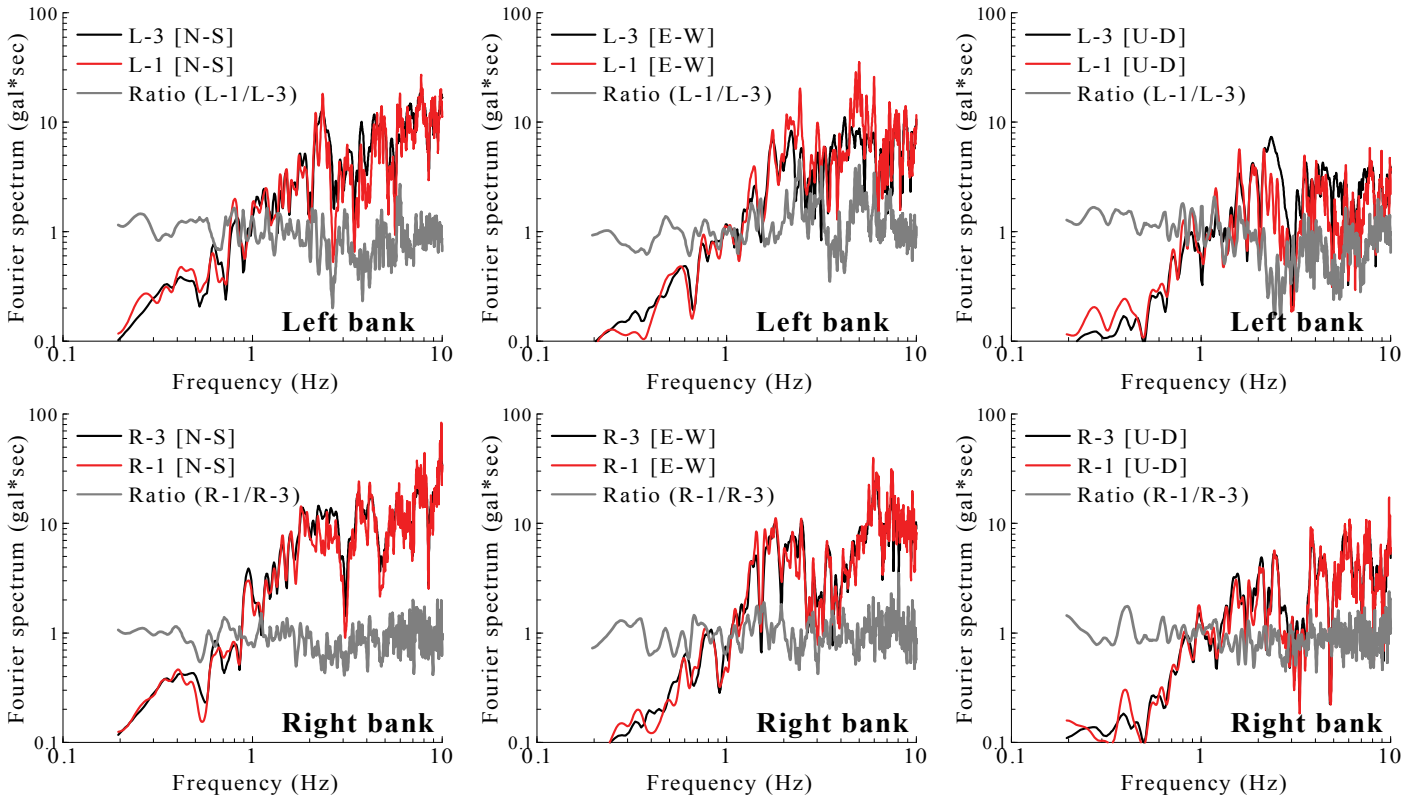


Fig. 7 Comparison of Fourier spectra of the observed ground motion due to Aftershock 2.

EVALUATION OF SITE EFFECTS

Site Amplification Factor

The distribution of permanent strong motion observation stations including K-NET, KiK-net and JMA stations is shown in Fig. 8. According to Fig. 2 and Fig. 8, KiK-net Ichinoseki-nishi is the closest permanent station to the bridge. No records are available for the station, however, during the period of temporary observation at the bridge sites. Therefore, the ratio of site amplification factors cannot be evaluated directly between KiK-net Ichinoseki-nishi and the bridge sites. On the other hand, EQ-01~07 were observed not only at the bridge sites but also at KiK-net Ichinoseki-higashi (see Fig. 9). The ratios of Fourier amplitude spectra between the bridge sites and KiK-net Ichinoseki-higashi are shown in Fig. 9 for EQ-01~07. To obtain the spectral ratios, the composition of two horizontal components was used and the spectra were processed through a Parzen window with a bandwidth of 0.05 Hz. In addition, the spectral ratios were corrected for the difference of hypocentral distance for the two stations (Boore, 1983; Satoh and Tatsumi, 2002). In Fig. 9, “mean ratio” indicates the mean of the spectral ratios due to EQ-01~07. The horizontal site amplification factors at the bridge sites were evaluated by multiplying conventional site amplification factor at KiK-net Ichinoseki-higashi (Nozu *et al.*, 2007) with the mean ratio. The site amplification factors at the bridge sites and surrounding strong motion stations are shown in Fig. 10. Some of the site amplification factors for permanent strong motion stations are based on Nozu *et al.* (2007) and others were obtained in a similar way as those at the bridge sites based on spectral ratios. The vertical site amplification factors were obtained based on horizontal-to-vertical spectral ratios.

In order to estimate strong ground motions at the firm ground outcrop (ISO23469), we carried out PS logging and soil density test at the temporary seismic observation sites (L-3 and R-3). The shallow soil profiles at the bridge sites are shown in Table 3. Then the site amplification factors from the bedrock to the surface at the bridge sites (Fig. 10) were divided by the theoretical transfer functions for the soil profiles to obtain site amplification factors at the outcrop of the firm ground (see Fig. 10). On the other hand, at KiK-net Ichinoseki-nishi and KiK-net Ichinoseki-higashi, surface-to-borehole spectral ratios were calculated based on vertical array records from moderate earthquakes before the main shock. Then the site amplification factors from the bedrock to the surface (Fig. 10) were divided by the average ratios to obtain site amplification factors at the depth of borehole seismometers.

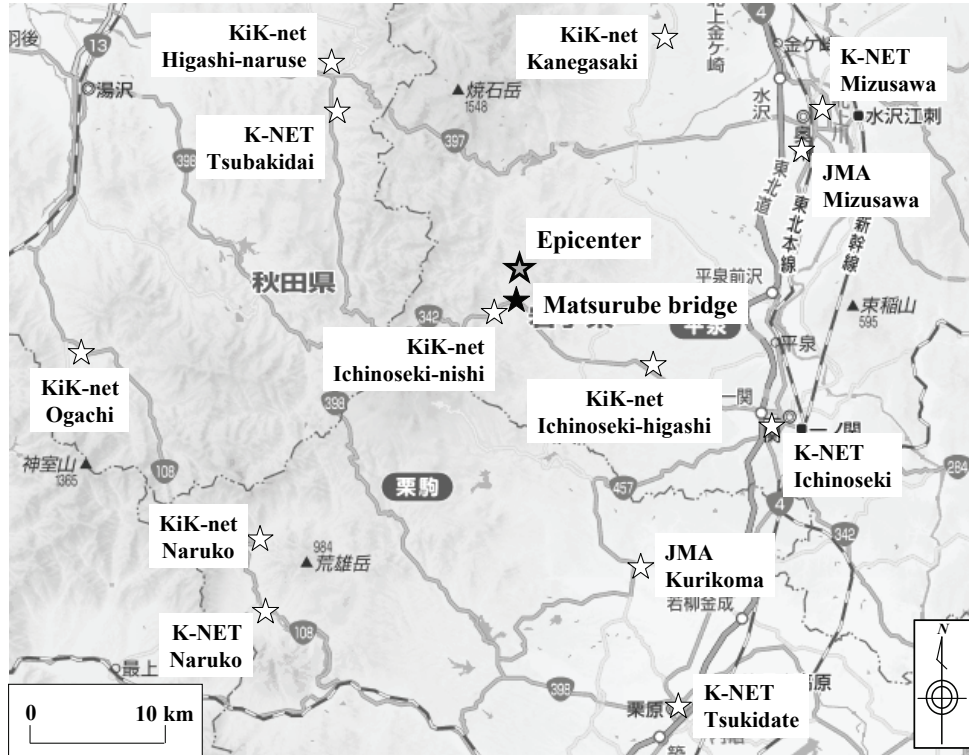


Fig. 8 Distribution of permanent strong motion stations around the Maturube Bridge.

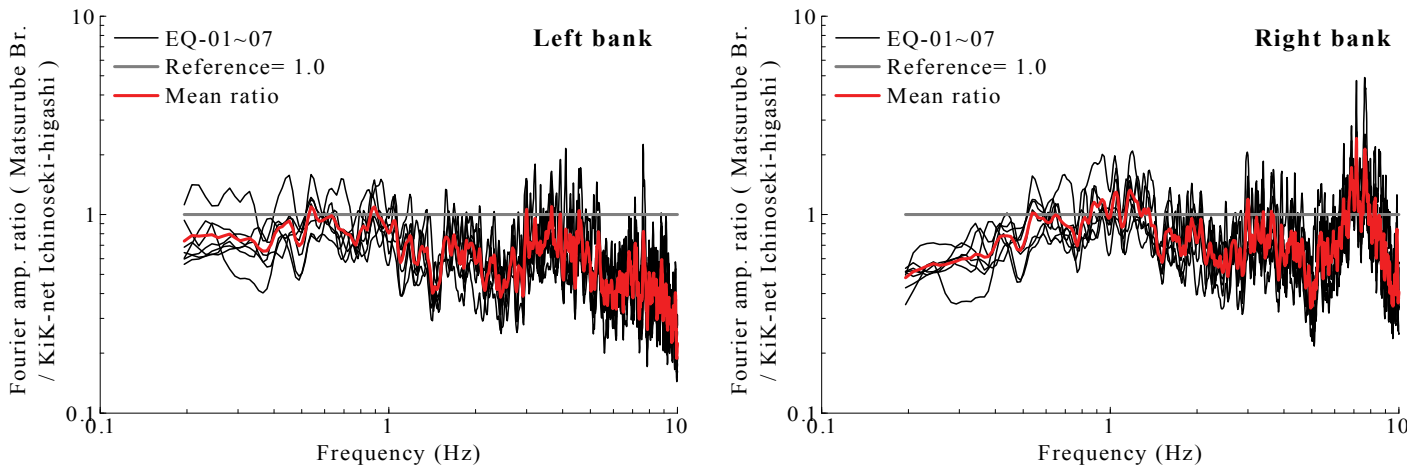


Fig. 9 Fourier spectral ratios between the bridge sites and KiK-net Ichinoseki-higashi, corrected for the difference of hypocentral distance

Table 3. Shallow soil profiles at the bridge sites.

(a) Left bank					(b) Right bank				
Soil layer	Depth (m)	Density (t/m ³)	P-wave velocity (m/sec)	S-wave velocity (m/sec)	Soil layer	Depth (m)	Density (t/m ³)	P-wave velocity (m/sec)	S-wave velocity (m/sec)
Surface soil	4.8	1.91	640	190	Surface soil	5.2	1.84	650	170
Bedrock		2.10	890	360	Sand and gravel	6.9	1.94	730	280
					Bedrock		2.12	880	390

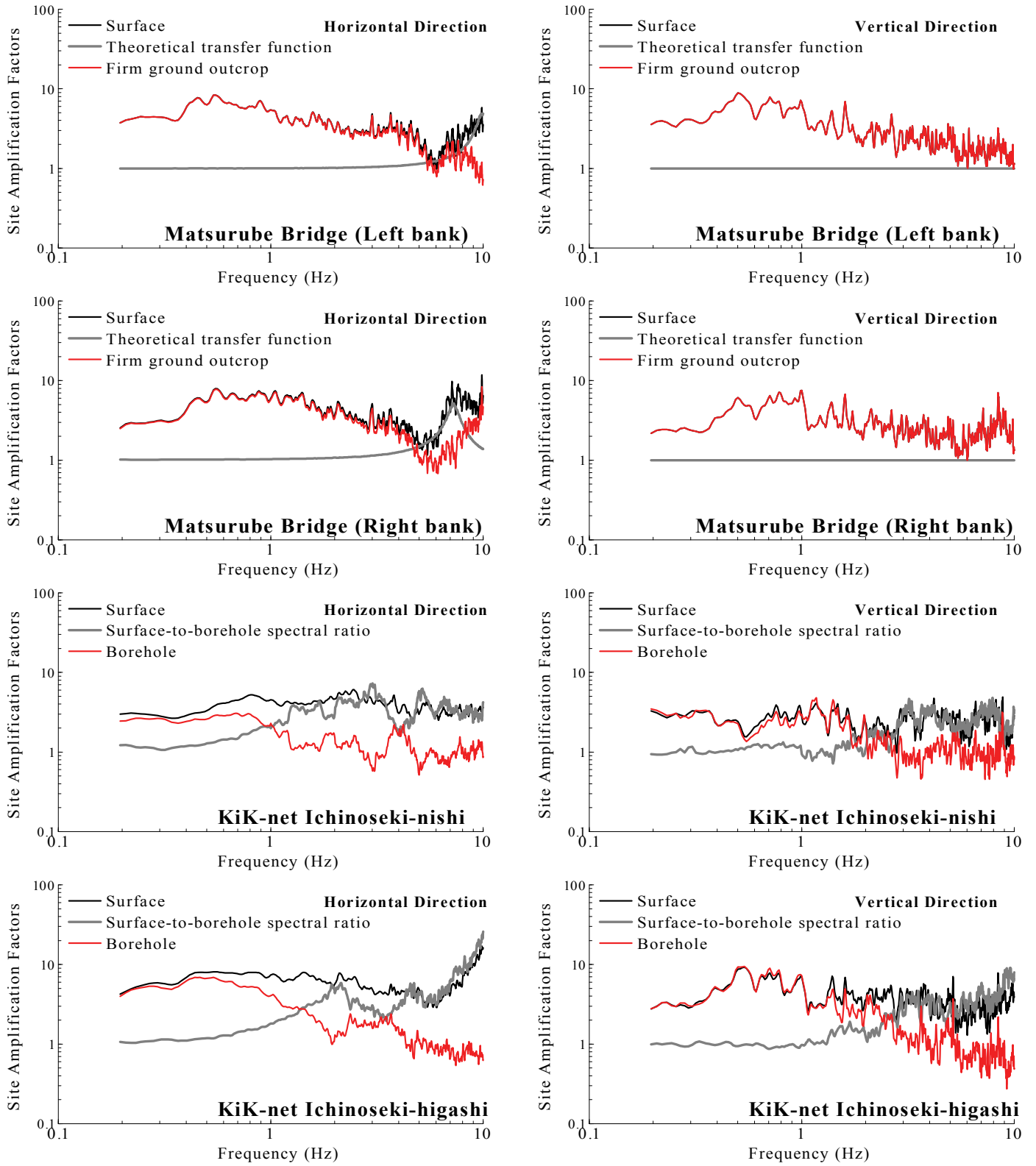


Fig. 10 Evaluation of the site amplification factors.

Site Phase Effect

The observed waveforms for Aftershock 1 were selected to be used for the evaluation of the site phase effect (Hata *et al.*, 2011). Appropriateness of this selection can be confirmed as follows. In Fig. 11, the observed velocity waveforms for the main shock of the

2008 Iwate-Miyagi Nairiku Earthquake (Mj7.2) at the permanent observation stations (see Fig. 8) are shown as black traces. On the other hand, the red traces indicate the synthetic velocity waveforms with the Fourier amplitude of the main shock and the Fourier phase of Aftershock 1. Both traces are band pass filtered between 0.2 and 2.0 Hz. In Fig. 11, we can recognize the similarity of the synthetic waveforms to the observed ones. Note that the two waveforms (black and red) in Fig. 11 have the same Fourier amplitude (that of the main shock) but different Fourier phase (that of the main shock or Aftershock 1). The similarity of the waveforms indicates that the record of the main shock and that of Aftershock 1 have almost the same Fourier phase for all the components, i.e., the Fourier phase of Aftershock 1 at the permanent stations is a good approximation of the Fourier phase of the main shock at the same stations. Thus, the Fourier phase of Aftershock 1 at the Maturube Bridge sites is used in the following estimation. The details of the evaluation of the site phase effects will be mentioned later.

STRONG MOTION ESTIMATION

Estimation Method

Fig. 12 shows the framework of strong motion estimation at the Maturube Bridge sites using the site effects substitution method (Hata *et al.*, 2011). The method is simply composed of 3 steps. First, the Fourier amplitude at the bridge sites for the main shock is evaluated by correcting the observed Fourier amplitude for the borehole seismometer at KiK-net Ichinoseki-nishi for the difference of the path effect (Boore, 1983; Satoh and Tatsumi, 2002) and the site amplification factors (see Fig. 10) at the bridge sites and KiK-net Ichinoseki-nishi. Here, the record at the ground surface of KiK-net Ichinoseki-nishi, which is affected by strong nonlinearity of local soil (e.g., Aoi *et al.*, 2008; Yamada *et al.*, 2009), was not used. Then, the Fourier phase at the bridge sites during the main shock is approximated by the Fourier phase for Aftershock 1 that occurred close to the main rupture area of the main shock. Finally, inverse Fourier transform is conducted to obtain causal time history (Nozu *et al.*, 2009) of strong ground motions at the firm ground outcrop at the bridge sites during the main shock. In order to confirm the validity of the estimation method, the strong ground motion for the borehole seismometer at KiK-net Ichinoseki-higashi for the main shock is evaluated by correcting the observed strong ground motion for the borehole seismometer at KiK-net Ichinoseki-nishi. The observed velocity waveforms and the evaluated velocity waveforms for the borehole seismometer at KiK-net Ichinoseki-higashi are compared in Fig. 13 for 3 components. The similarity of all traces indicates the applicability of the estimation method.

Strong Motion Estimation

Fig. 14 and Fig. 15 show the estimation results of velocity and acceleration waveforms at the firm ground outcrop at the bridge sites. Here, the velocity waveforms are band pass filtered between 0.2 and 2.0 Hz. The peak ground accelerations for the composition of 3 components at the firm ground outcrop of the left bank and right bank are 1,560 gal and 1,347 gal respectively. The JMA seismic intensity at the firm ground outcrop of the left bank and right bank are 6.3 and 6.2 respectively. It should be noted that, in the estimation process, it is assumed that the firm ground outcrop motion is not affected by soil nonlinearity. Fig. 16 is the comparison of the design response spectra (Damping: 5%) by Specifications for Highway Bridges (SHB) and the estimated acceleration response spectrum (Damping: 5%). The ground at the bridge sites can be classified as type-I in the specification. For frequencies lower than 2.6 Hz, the estimated spectra are smaller than the design spectrum. Because the natural frequency of the Maturube Bridge is 1.7Hz (Sakai *et al.*, 2010), it is likely that the inertia force on the structure during the 2008 event was not the main cause of the failure of the bridge.

CONCLUSION

The strong ground motions at the Maturube Bridge sites due to the 2008 Iwate-Miyagi Nairiku Earthquake (Mj7.2) were evaluated based on the site effects substitution method. As a result, it was found that, around the natural frequency of the bridge, the acceleration spectra did not exceed the design response spectrum by Specifications for Highway Bridges. Therefore, it is likely that the inertia force on the structure during the 2008 event was not the main cause of the failure of the bridge. In the future study, the estimation results will be further confirmed by conducting a strong motion simulation using a characterized source fault model.

ACKNOWLEDGEMENT

Strong motion data of KiK-net were kindly provided by the National Institute for Earth Science and Disaster Prevention through the website at www.kyoshin.bosai.go.jp (last accessed June 2011). The authors thank the local government of Ichinoseki City for cooperating in the aftershock observation and microtremor measurements at the Maturube Bridge sites.

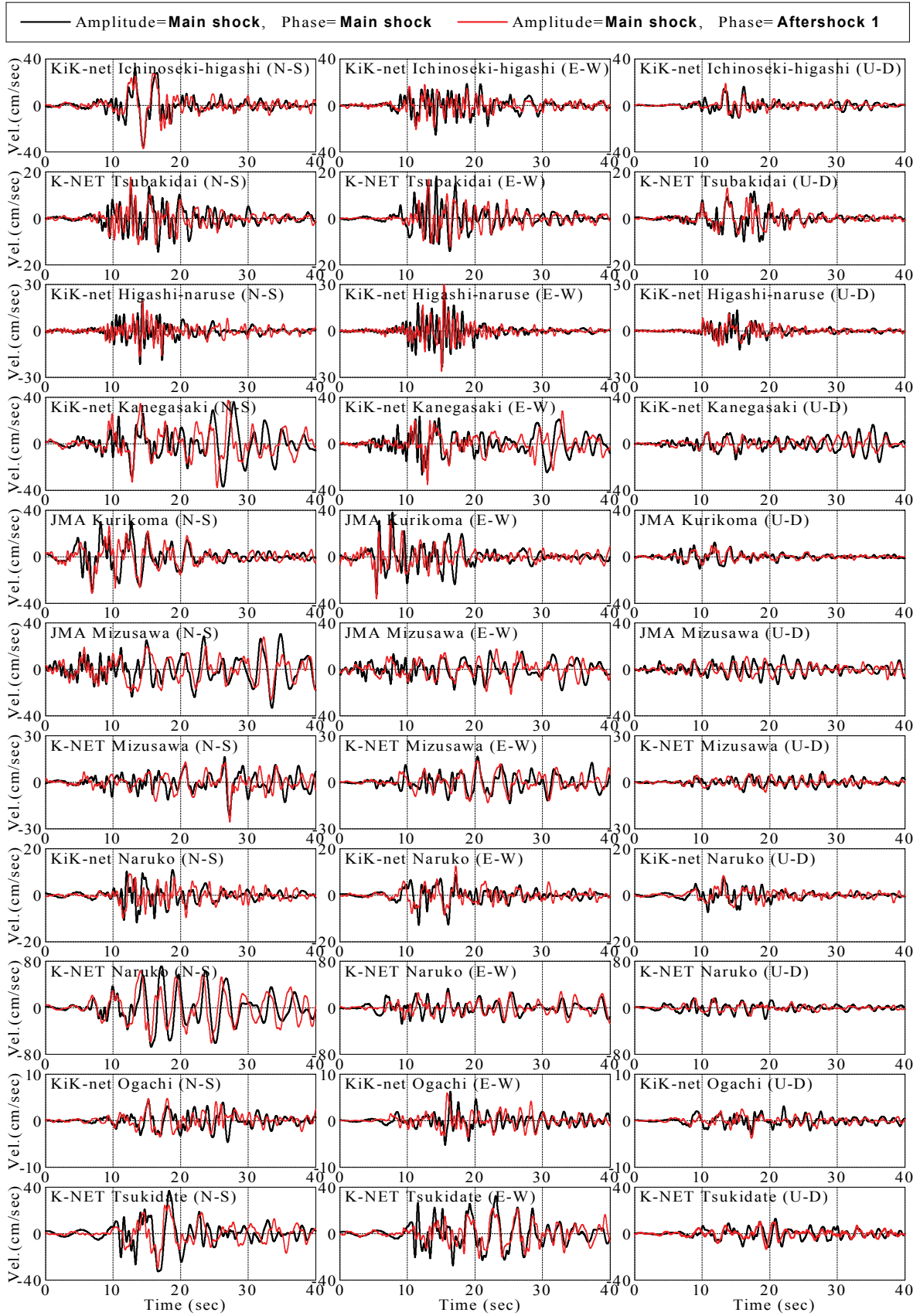


Fig. 11 Confirmation of the validity of site phase effect evaluation.

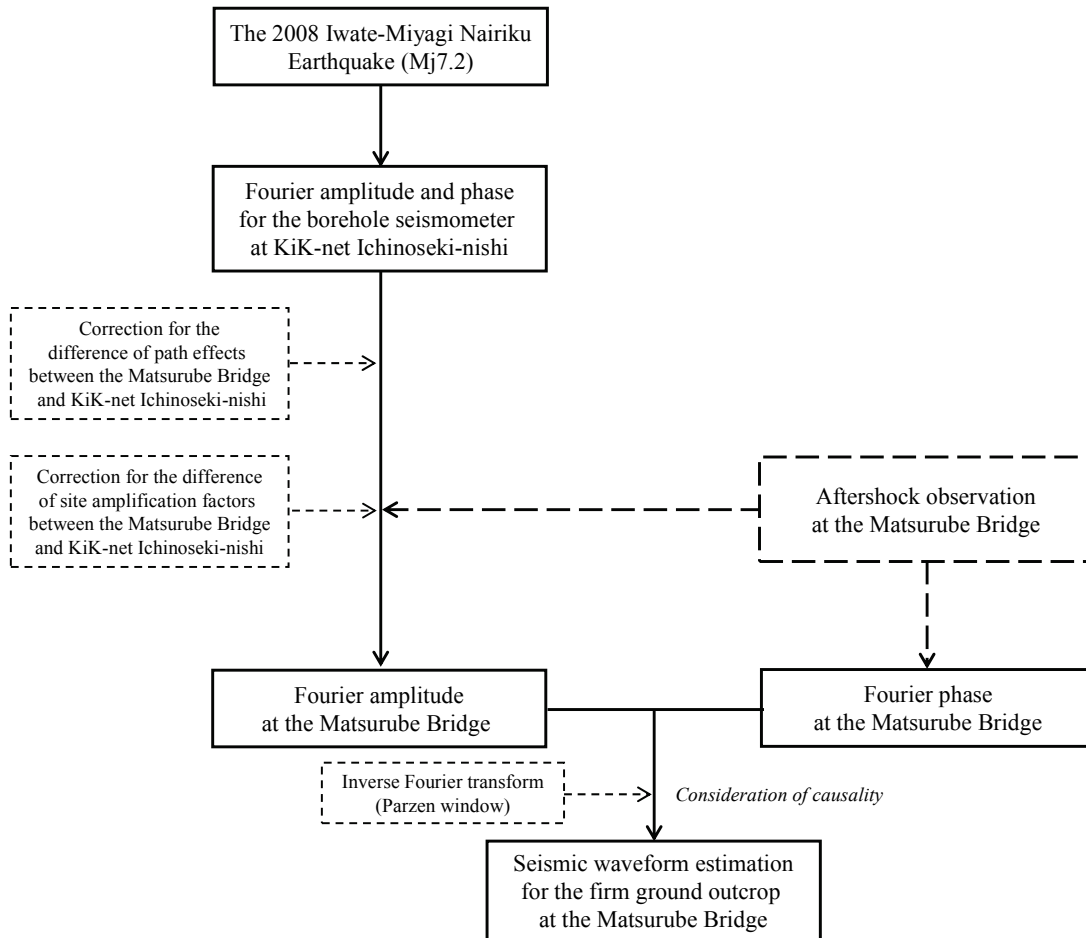


Fig. 12 Framework of the strong motion estimation method.

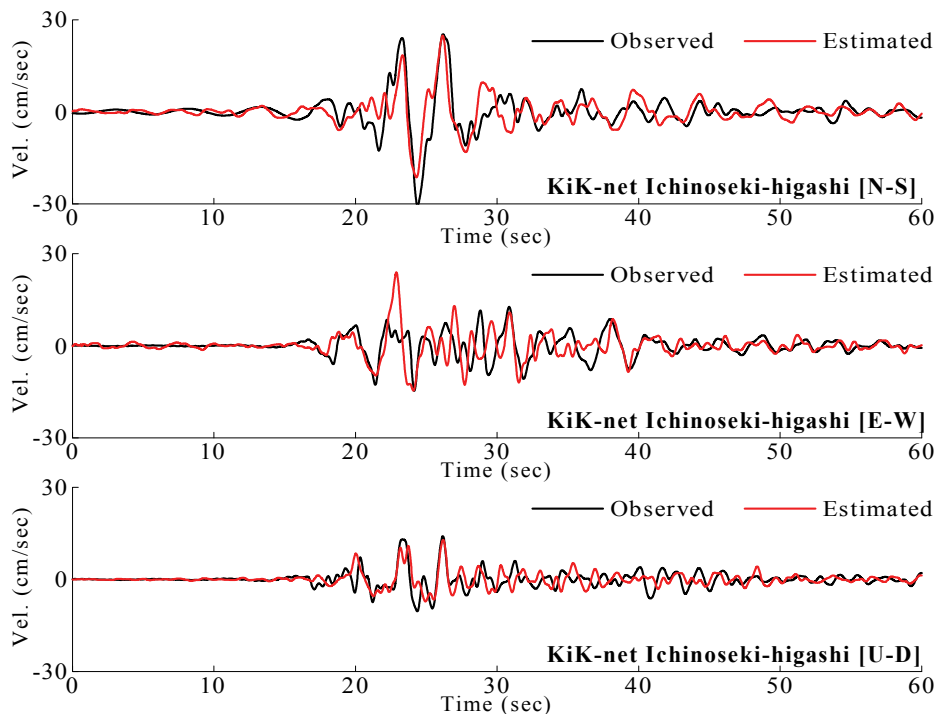


Fig. 13 Confirmation of the validity of the strong motion estimation method.

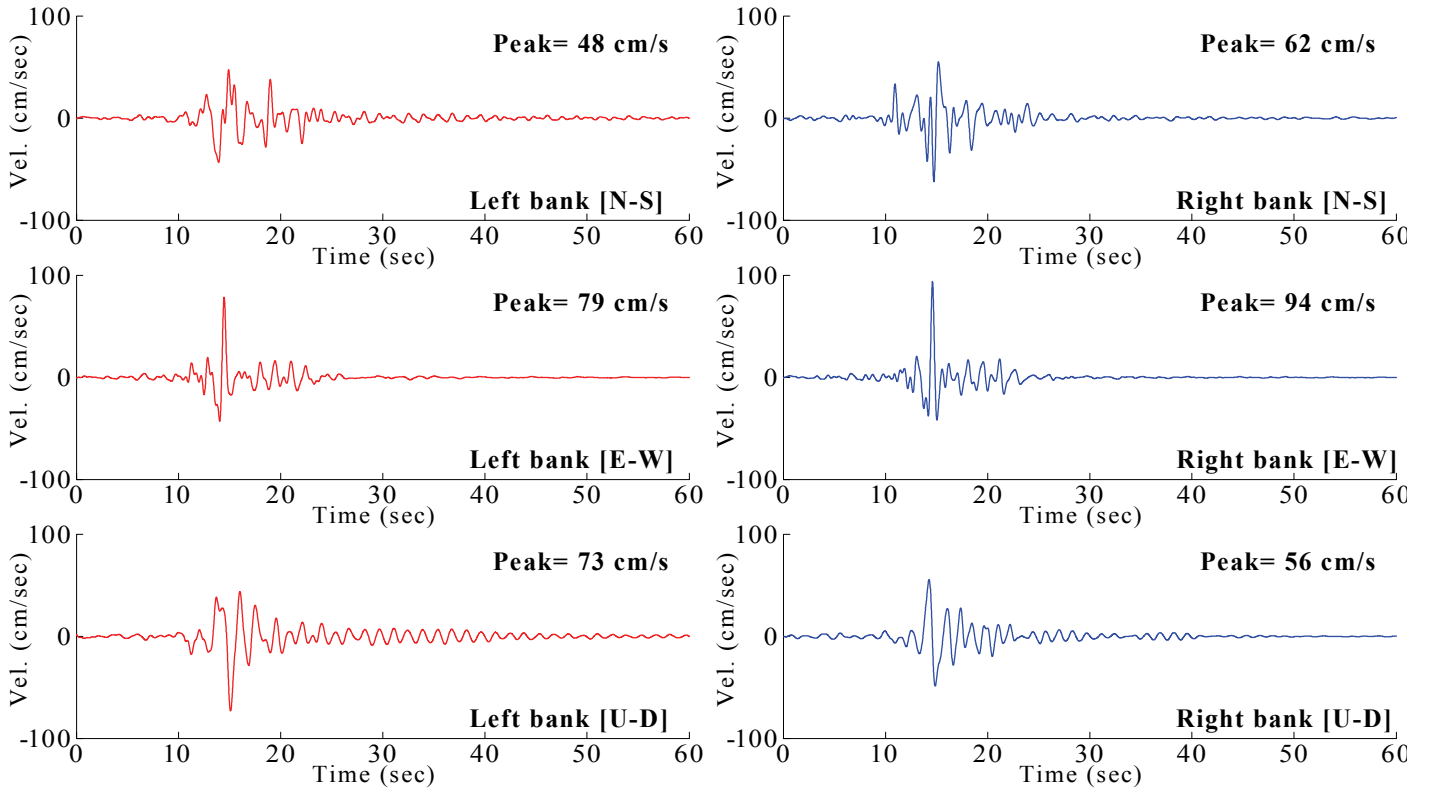


Fig. 14 Estimated velocity waveforms at Matsurube Bridge during the main shock.

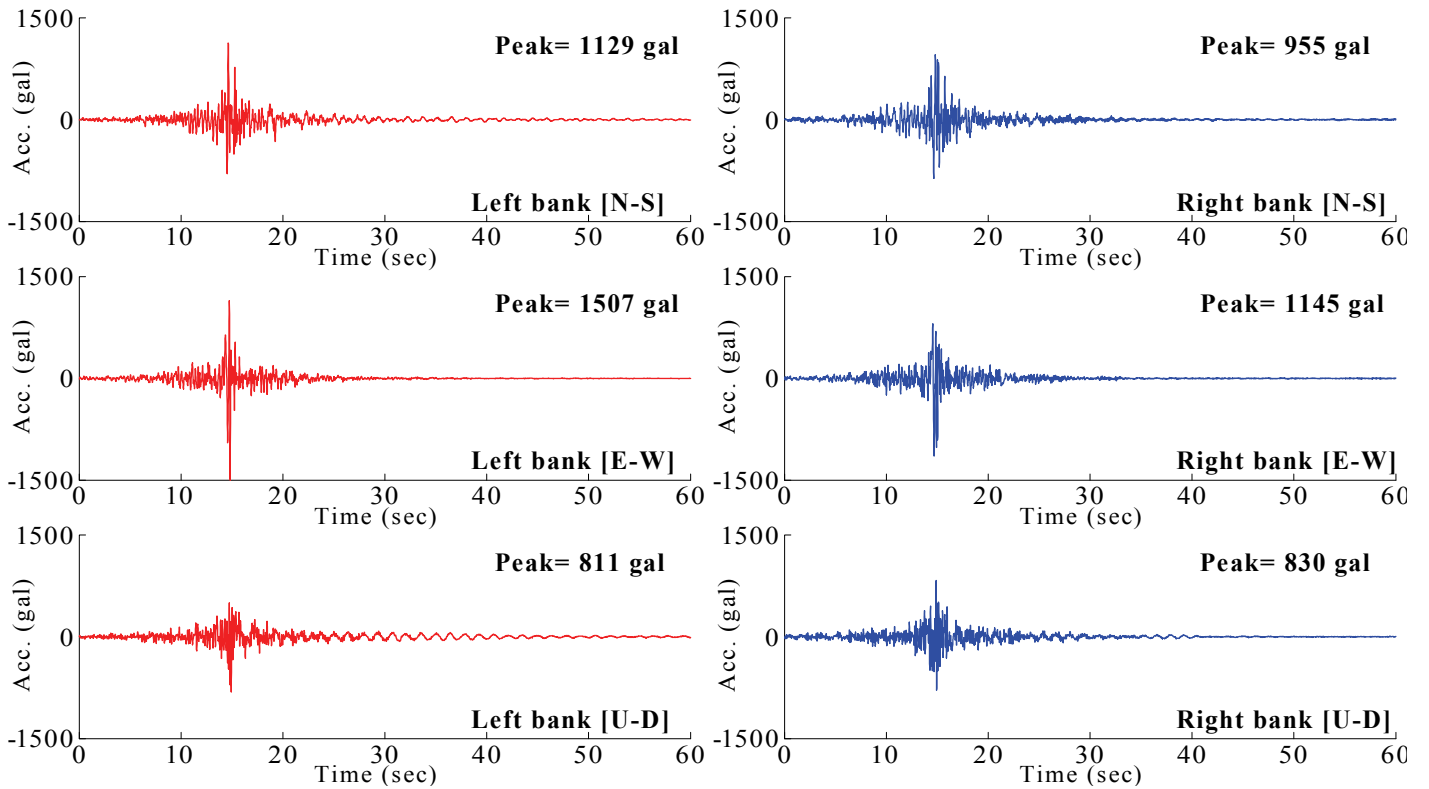


Fig. 15 Estimated acceleration waveforms at Matsurube Bridge during the main shock.

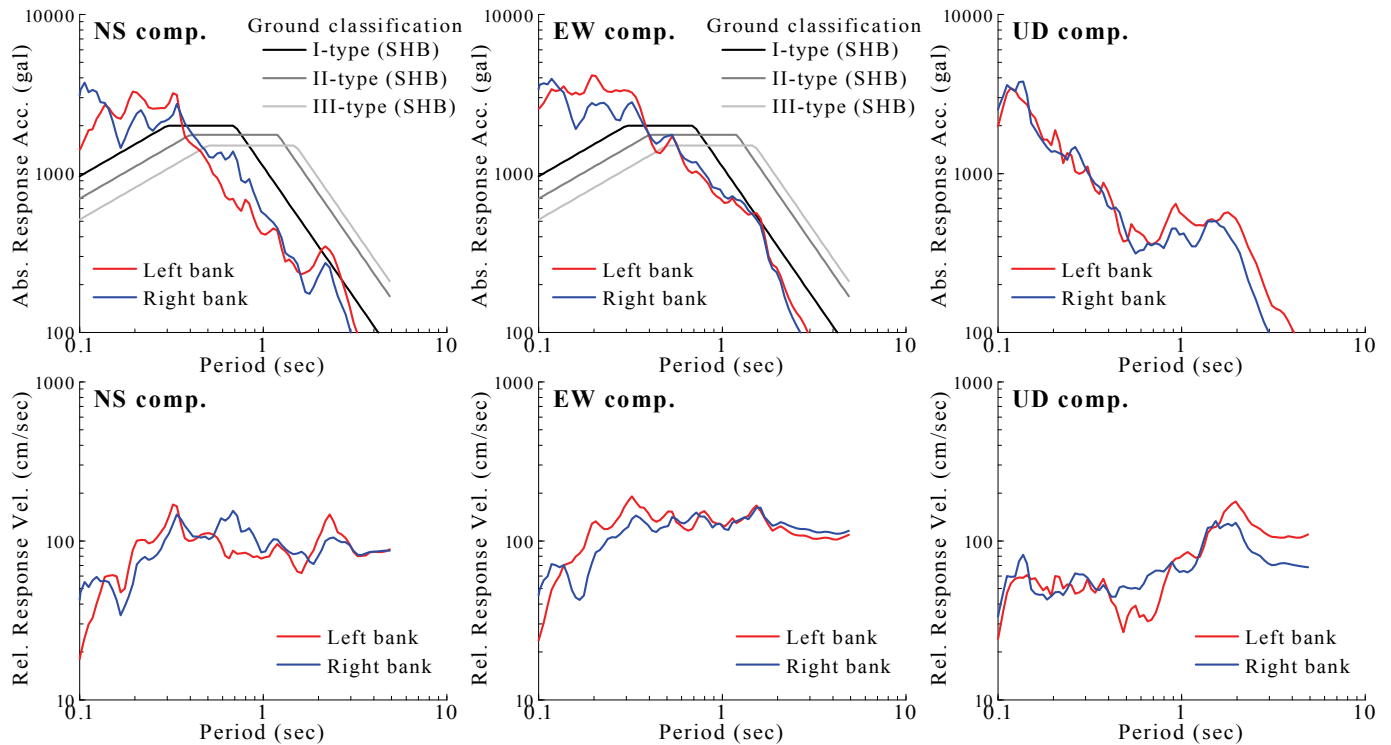


Fig. 16 Response spectra of the estimated strong motions at Maturube Bridge sites.

REFERENCES

- Aoi, S., T. Kunugi, and H. Fujiwara [2008], "Trampoline Effect in Extreme Ground Motion", *Science*, Vol. 322, pp. 727-730.
- Boore, D.M. [1983], "Stochastic Simulation of High-Frequency Ground Motions based on Seismological Models of the Radiated Spectra", *Bulletin of the Seismological Society of America (BSSA)*, Vol. 73, No. 6A, pp. 1865-1894.
- Hata, Y., S. Nakamura, A. Nozu, S. Shibao, Y. Murakami, and K. Ichii [2010], "Microtremor H/V Spectrum Ratio and Site Amplification Factor in the Seismic Observation Stations for 2008 Iwate-Miyagi Nairiku Earthquake", *Bulletin of the Graduate School of Engineering, Hiroshima University*, Vol.59, No.1.
- Hata, Y., A. Nozu, and K. Ichii [2011], "A Practical Method to Estimate Strong Ground Motions after an Earthquake Based on Site Amplification and Phase Characteristics", *Bulletin of the Seismological Society of America (BSSA)*, Vol. 101, No. 2, pp. 688-700.
- Nozu A., T. Nagao, M. Yamada [2007], "Site Amplification Factors for Strong-Motion Sites in Japan Based on Spectral Inversion Technique and their Use for Strong-Motion Evaluation", *Jour. of Japan Assoc. Earthq. Eng.*, Vol. 7, No. 2, pp. 215-234 (in Japanese with English abstract).
- Nozu, A., T. Nagao and M. Yamada [2009], "Simulation of Strong Ground Motions Using Empirical Site Amplification and Phase Characteristics: Modification to Incorporate Causality", *Jour. of Japan Soc. Civil Eng. A*, Vol. 65, No. 3, pp. 808-813 (in Japanese with English abstract).
- Sakai, J., S. Unjoh, J. Hoshikuma and G. Zhang [2010], "A Study on the Damage and the Seismic Response Characteristics of Maturube Bridge due to the 2008 Iwate-Miyagi Nairiku Earthquake", *Proc. of the 3rd Symposium on Recent Damaging Earthquakes around the World*, Vol. 3, No. 17, pp. 107-114 (in Japanese).
- Satoh, T. and Y. Tatsumi [2002]. "Source, Path, and Site Effects for Crustal and Subduction Earthquakes Inferred from Strong Motion Records in Japan, *Jour. of Struct. Constr. Eng.*, AIJ, No. 556, pp. 15-24 (in Japanese with English abstract).
- Yamada, M., J. Mori and T. Heaton [2009], "The Slapdown Phase in High-acceleration Records of Large Earthquakes", *Seismological Research Letters*, Vol. 80, No. 4, pp. 559-564.